Silicon Nanocrystals: From Synthesis to Applications

R. Karmouch

Jazan University, Physics Department, Jazan, P.O BOX 2097, KSA

Abstract—The reduction in size to nanoscale sizes not only allows to improve the performance but also to bestow new properties to materials; this is what justifies the growing interest in this type of materials such as the silicon nanocrystals that are fully compatible with existing technologies we can expect to see an explosion of applications based radically on the silicon nanocrystals in disciplines such as biology, mechanics, electronics… The specificity of nc-Si resides essentially in the influence of their size and their shape. However, the n-Si must have controlled properties, both from the point of view of a single particle or of a set of interacting particles in an amorphous matrix. Thus, it is of great technological and scientific interest to know the physical and chemical properties of Si nanocrystals, different methods of nc-Si production, the methods of their characterization and their applications in microelectronics, optoelectronics and biophotonics.

Index Terms—Silicon nanocrystals, Synthesis, properties, and applications in in microelectronics, optoelectronics, biophotonics.

1 Introduction

The bulk crystalline silicon is today the most widely used in the microelectronics and photovoltaic industry material. Indeed, miniaturization the IC components, the increase in their operating speed, as well as the decrease of the transistors production costs and other elements of the microelectronics over the years are unprecedented in the history of mankind. According to Intel Company during the forty recent years, the number of integrated transistors contained in the various processors manufactured is increased exponentially, which mean that the number of transistors per processor double approximately every 18 months, according to Moore's Law, set out in 1965 by the co-founder of the firm Intel, Gordon E. Moore [1]. The assessment, entitled International Technology Roadmap for Semiconductors (ITRS), updated annually by many actors semiconductor industry [2], identifies many obstacles that will face the IC manufacturers in coming years. In particular, the interconnections in integrated circuits [3] and no solutions available by using the current technology especially that the growth of total length of 2010, will reach the astronomical value of 2000 m /cm^2 (and 4000 m/cm^2 in 2015) one possible solution to overcome this problem is the use of the optical interconnects. In recent years, reducing the size of the Si nanoscale brought new capabilities that allowed numerous applications in optoelectronics based on (nc-Si) silicon nanocrystals such as the optical interconnection [4], non volatile memory [5], and Third Generation Photovoltaic Solar Cells. [6] This research field generated a very strong passion for research in the last ten years. According to the Google ScholarTM the number of publications related to nc-Si is 122,000 articles published between 1990 and 2016. [7] In particular, nanocomposite materials with Si-nc embedded in an amorphous dielectric matrix have been a significant number of publications. Three application areas driving these studies: optical

systems that rely on the emission properties of nc-Si in the visible and at room temperature, non-volatile memories interested in electric charging properties of nc -Si, and photovoltaic systems such as multi-junction Si-nc cells based on quantum confinement phenomena in nc-Si. [8]

The manufacture of silicon nanostructures is fully compatible with existing technologies. However, to be successfully integrated into the opto- and microelectronic devices, the n-Si must have controlled properties, both from the point of view of a single particle as a set of interacting particles in an amorphous matrix. A particle can be represented in a simple way from its volume and its surface whose properties are distinct. Indeed, with the reduction in the size of the nanostructures, the surface/volume ratio increases drastically and surface phenomena become more pronounced. In other words, the physicochemical properties of nc-Si are strongly influenced by the nature of the surface and interfaces. [9] Up to now the origin of light emission from nc-Si is still a big debate between scientists. Many studies focus on the impact properties of nc-Si without considering the influence of the surrounding matrix. Nevertheless, many parameters such as the chemical nature of the latter, the concentration and type of defects, mechanical stresses imposed by the network can influence profoundly the optoelectronic properties of the material at the microscopic and macroscopic scale. It is therefore essential to have a better understanding of these phenomena.

In this spirit, this work is devoted to review techniques used for the fabrication of silicon nanocrystals, the origin of luminescence of nc-Si, and their application in optoelectronics.

A remind of the basic properties of silicon will be of great importance to understand well the silicon nanocrystals properties.

2 PHYSICAL PROPERTIES OF SILICON

Silicon is, on Earth, the most abundant element after oxygen; we estimates that the Earth's surface is composed about 26% of silicon. [10] This tetravalent metalloid, has an atomic number of 14, and an atomic mass of 28.0855 u.a, and has the diamond crystal structure which is the combination of two face centered cubic structures having an offset of a quarter of the length of the diagonal from each other along the diagonal of the cube with a lattice parameter a = 5.43 Å to the room temperature, each atom has four nearest neighbors. Table 1; summarizes the main properties physical Si. The analysis of the band structure of the semiconductor material reveals an indirect band gap (or indirect gap) width Eg equal to 1.12 eV at room temperature, as shown in Figure 1. Also, the pairs of recombination electron-hole in the crystalline silicon requires the presence of a phonon, which makes it unlikely, and the estimated recombination rate is about 10^2 s^{-1}, compared to $2x10^7$ s^{-1} in gallium arsenide (GaAs) that has a direct gap. [11] Thus the lifetime of radiation corresponding to recombinations is of the order of a millisecond for the Si and nanosecond only for GaAs. This is reflected directly in the luminescence efficiency, which is only 10^{-4} to 10^{-5} for the crystalline Si, compared to 10^{-1} for a direct gap semiconductor. [12]

Propriété	Valeur	Description
a	0.5431 nm	Paramètre de maille (300 K)
ρ	2.329 g/cm^3	Densité
E_g	1.12 eV	Largeur du gap (300 K)
E_g	1.17 eV	Largeur du gap (0 K)
Δ_0	0.044 eV	Couplage spin-orbite
χ	4.05 eV	Affinité électronique
m_{hh}	0.49	Masse relative des trous lourds
m_{lh}	0.16	Masse relative des trous légers
m_L	0.916	Masse relative des électrons longitudinaux
m_T	0.19	Masse relative des électrons transverses
μ_n	0.15 m^2/Vs	Mobilité des électrons (300 K)
μ_p	0.045 m^2/Vs	Mobilité des trous (300 K)
ε_{rel}	11.7	Constante diélectrique relative
n	3.42	Indice de réfraction statique
T_m	1685 K	Température de fusion

Table 1: Principals physical properties of crystalline silicon.

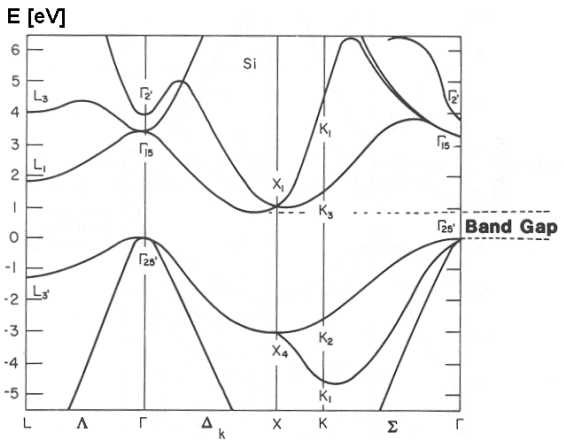

Figure 1: Silicon band structure in the directions X(100) and L(111).

3 SILICON NANOCRYSTALS

One can then understand why the choice of bulk Si for obtaining sources effective light for applications in optoelectronics was never considered seriously. Moreover, it is certainly the same reasons that hindered for many years the development of photonics based on silicon while the progress of the same material in the field of microelectronics was very successful. The prospects around silicon as a light source has drastically changed in 1990 after Canham [8] discovered the intense photoluminescent emission (PL) in the visible range produced by an etched Si substrate. The wavelength of this emitted light could sweep the spectral range of the visible by simply changing the anodizing conditions and that the luminescence efficiency could reach 10% in the most favorable case. The various analyzes have shown that the luminescence originated from the etched layer that consist of an interposed network of "columns" of Si and pores which gave its name to silicon porous (p-Si). In fact, at the microscopic level, the p-Si consists of small crystallites (typically a few nanometers in diameter) of varied shape corresponding to Si- nanocrystals. The first publications on the subject, suggested that when the crystals dimension are reduced to nanoscale size, they then become good light emitters under the action of an optical excitation [13, 14], or electrical excitation (electroluminescence) [15, 16]. In fact, the reduced dimensions of the crystal structure of bulk Si to nanoscale will cause very significant changes in their optoelectronic properties. To better understand these effects it is useful to recall some concepts of quantum mechanics for a confined system. In general a confined system is one in which a particle (an electron for example) is localized in a potential well, surrounded by infinite potential barriers. Confinement effects will be present when the size of the confinement will be of the order of the spatial extension of the wave function of the particle. In a confined system, the energy of electronic states increases with the confinement condition. The result therefore is a discretization of the energy forming the energy levels of system represented by the following expression:

$$E_n = \frac{n^2\pi^2h^2}{2mR^2} \qquad (1)$$

where m = mass of the particle, R is the width of the well.

The effects of confinement for a nanocrystal semiconductor is the widening of the bandgap and an increase in the probability of irradiative transitions and this become significant when the magnitude of the Bohr radius of the exciton and the radius of the nanocrystal (R) become comparable.

For the case of silicon, Xia *et al.* [18] and Yoffe *et al.* [19] found that when the radius of the nc-Si approaches the 5 nm the effects of a strong quantum confinement of carriers begin to appear. Up to now many works are published on the electronic states calculation within nc-Si. A summary for these calculations was published by John *et al.* and Singh *et al.* in 1995 [20].

4 METHODS FOR NC-SI SYNTHESIS

The discovery of the visible luminescence from p-Si discussed in the previous section caused a particular interest to find other methods than chemical etching to obtain nc-Si. Among these methods which may be mentioned includes: Ion implantation of Si ions in host matrices [21], the chemical deposition vapor phase of layers of non-stoichiometric oxide SiO_x (1 <x <2) (LPCVD) [22], the reactive sputtering of a Si substrate in an oxidizing atmosphere to form the layer non-stoichiometric oxide (sputtering) [23], laser ablation of a Si substrate [24], the attack a Si substrate by electrical impulses (spark method) [25], the deposition of clusters by decomposition of silane gas [26] or the recrystallization of amorphous silicon layers. [27]

4.1 Ion implantation

Among the fabrication methods of nc-Si we find the ion implantation that is considered as one of the most promising because it's compatible 100% with the technological process of the current microelectronics. The main advantage of this technology compared to the etching method to obtain p-Si is the high thermal and chemical stability of nanostructures since they are

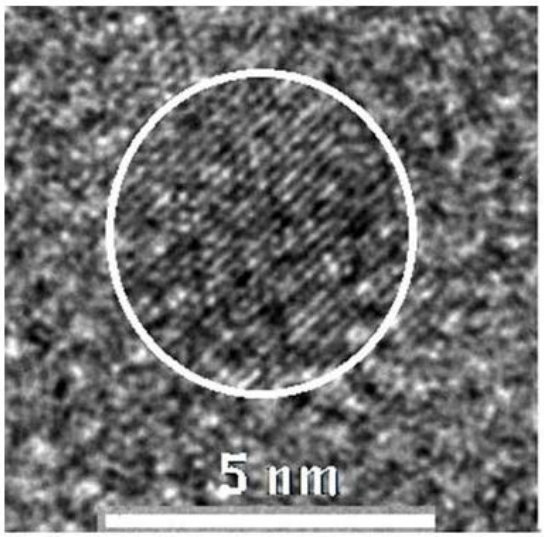

surrounded by a passivating host matrix.

Figure 2: HRTEM image for the nc-Si embedded in SiO2 matrix. [17]

The nc-Si obtained by ion implantation process are of good quality as shown in the image in Figure 2 obtained by (HRTEM) of a nanocrystal immersed in a 40 nm thick SiO_2 layer. The nc-Si diameter is less than 5 nm as shown by the circled area. [17, 21, 28]. The process begins with an ion implantation of Si^+ in a layer of SiO_2 previously deposited thermally on a substrate. The process is

then followed by an annealing at temperatures above 900 °C and for 100 minutes in a mixture of nitrogen and hydrogen atmosphere [29] to ensure at the same time a good demixing of phases of the system Si/SiO_2 and passivation of defects created in the matrix when implanted.

The nc-Si density, their average size and its dispersion is determined by a number of factors, and the most important are the initial level of supersaturation of Si in the implanted matrix and the subsequent thermal annealing conditions. While these factors can explain rather adequate changes in the population of nanocrystals, another very important factor also plays a role in modifying the nc-Si population is the annealing atmosphere. In 1996, Wendler *et al.* [30] published a study on the influence of heat treatment conditions on silicon nanocrystals. He found that under oxidizing atmosphere, the oxidation front advances from the surface toward the maximum concentration of precipitates (Figure 3a), which causes obviously a reduction in the concentration of excess Si within the implanted matrix. However, when the annealing is under a non-oxidizing atmosphere (Figure 3b) only a slight surface oxidation occurs of the implanted layer and accompanied with a simple redistribution of Si atoms in excess. Thus, according to this study, it is generally considered that the facts the annealing in an oxidizing atmosphere after the formation of silicon nanocrystals will reduce the number of excess silicon in the matrix and therefore reducing both the size and density of the nc-Si agglomeration.

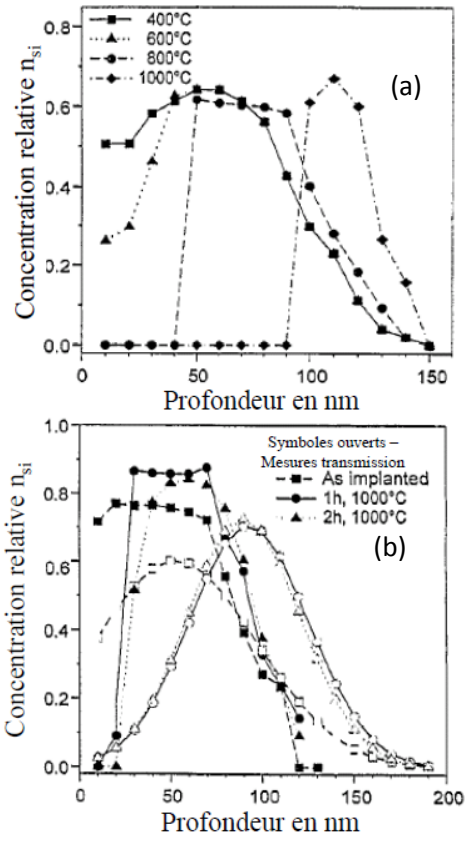

Figure 3: Comparison between implantation profiles for annealing a) oxidant atmosphere and b) non-oxidant one. [30]

In contrast, the annealing under nitrogen modify only the size of the nanocrystals (Ostwald ripening) [31] without significantly modifying their density.

Several studies have shown that passivation with hydrogen at temperatures around 500 °C increases the intensity of the luminescence of nc-Si by about a factor of 10. [32] The weakness of the luminescence before passivation is attributed to defects in the form of pendant bonds in the nanocrystal or their interface with SiO_2. Indeed, such defects are non-radiative recombination sites. [33] The energy is then emitted as phonons rather than contributing to the PL. During the passivation process, hydrogen diffuses into the sample and

acts on the pendants links, preventing such signal losses.

In summary, ion implantation allows for proper control of size distribution of nc-Si with sometimes comparable luminescence yields to those obtained on p-Si.

4.2 LPCVD

The LPCVD technique is one way of chemical deposition in vapor phase and it's among the most used techniques for the production of devices such as MOSFETs, thin film transistors or solar cells. In 1996, Nakajima *et al.* [22, 34] were among the first to apply this technique for the development of nc-Si. Two main methods can be identified for obtaining the silicon nanocrystals using this technique:

4.2.1 Deposited silicon nanocrystals:

This method consists in making a deposit of nc-Si on an insulating layer (SiO_2 or Si_3N_4) from the thermal decomposition of pure silane (SiH_4) at a temperature of around 600°C, the chemical reactions that govern the growth of silicon nanocrystals are described by the following equations:

$$SiH_4(g) \rightarrow SiH_4(s) \rightarrow S(s) + 2H_2(g) \quad (2)$$

$$SiH_4(g) \rightarrow SiH_2(s) + 2H_2(g) \rightarrow Si(s) + 2H_2(g) \quad (3)$$

In the range of low pressures, adsorption and dissociation of SiH_4 on the surface (equation 1) predominate and the role of radical SiH2 resulting from pyrolysis of SiH_4 (equation 2) is negligible. A descriptive scheme of this method is shown in figure 4 a) as well as a typical SEM image of the nc-Si in b). The concentration of the silicon nanocrystals, their size and their dispersion depend mainly on the temperature of the deposit and the silane pressure in the chamber.

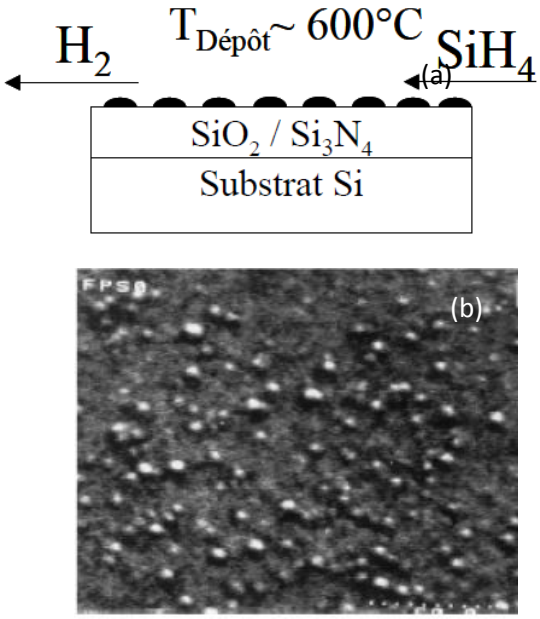

Figure 4: a) sketch of the process of nc-Si deposition b) image of nc-Si islets [35]

4.2.2 Precipitated silicon nanocrystals:

This second method was widely studied by Hitchman *et al.* [36] and consist to obtain nc-Si by precipitation of Si atoms in excess in a non-stoichiometric oxide layer (SiO_x, x<2). The reaction of SiH_4 and N_2O at the surface of the thermal SiO_2 layer causes the formation of a non-stoichiometric oxide layer (SiOx, x<2) rich in silicon, this layer is then annealed to separate the SiO_x phase to Si and SiO_2 giving as a final result the formation of nc-Si by precipitation as shown in the figure 5.

In this case the concentration of the nanocrystals, their size and their dispersion depend on the ration of N_2O/SiH_4, the temperature, and the subsequent thermal annealing. The main advantage of this

technique is the high chemical and thermal stability obtained by the passivation provided by

the surrounding matrix (SiO_2). The LPCVD technique allows a better control of the size distribution of the crystallites similar to the ion implantation but the reported luminescence efficiencies are significantly lower than those observed on the p-Si or nc-Si obtained by ion implantation.

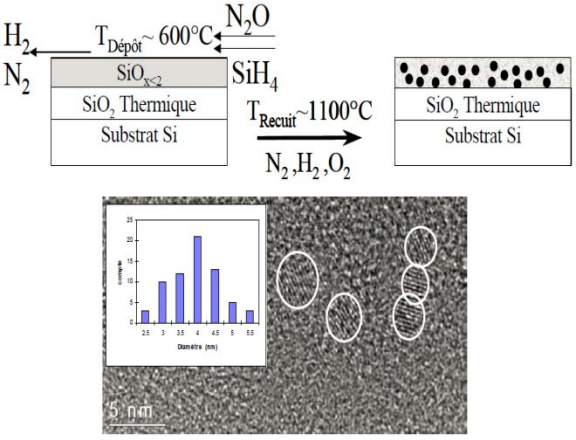

Figure 5: Diagram for obtaining nc-Si by precipitation in oxide layer by LPCVD. TEM image in plan view to determine the size and the distribution of nc-Si. [36]

4.3 Sputtering

This technique consists to use a magnet (Magnetron) placed behind the deposition source (target) that is negatively biased. The magnetic field generated by the magnetron will cause the formation of a closed annular field lines at the target surface thereby increasing the product of the ionization probability of the sputtering reaction in the confinement zone as illustrated in Figure 6. [23] To obtain the nc-Si using this technique, one can use two methods. The first method (co-sputtering) involves the use of two targets (SiO2 substrate + Si substrate) placed in the same room with a Si substrate under argon atmosphere. The second method (reactive sputtering) involves the use of a single target (Si substrate) placed in the same room with the substrate under Ar/O_2. In both cases we obtain a non-stoichiometric oxide SiO_x ($1 < x < 2$) layer on the Si substrate, which is then annealed to precipitate the silicon nanocrystals.

In this technique, the control of the size distribution of nc-Si is rather poor and the luminescence efficiency is also significantly lower

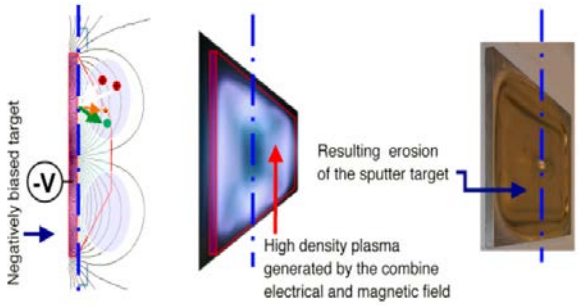

than that of p-Si.

Figure 6 - Operation Principle of the spray system. [23]

4.4 Laser ablation (PLD)

The silicon nanocrystals are obtained through condensation of the material resulting from laser ablation in a jet of high gas pressure. [24, 37] The size distribution depends on the pressure, the nature of the gas and the power of the laser excitation. A classic picture of the PLD deposition chamber is illustrated in the figure 7.

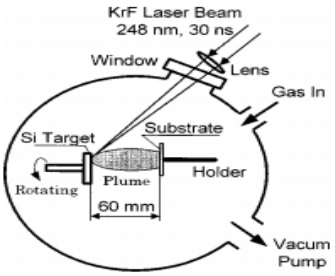

Figure 7: Schematic of PLD system

The process begins with a laser that focus a spot with an angle of 45° on a rotatable target, and then the deposit is collected on a substrate previously placed of preference perpendicularly to the target with a typical distance of 30 mm. The duration of the deposition is controlled by the number of the laser pulses. This technique allows a better control of the size distribution of the nc-Si but the yield of luminescence is lower than the obtained one with p-Si.

4.5 Spark process

The production of nc-Si by this technique is relatively simple and the structure of the layer is very similar to that obtained by etching the silicon substrate (p-Si). [25] The setup of this technique comprises a typical electrode placed at a distance of 1 mm from the silicon substrate that applies for a specified time a certain amount of electric pulses with high-frequency (a few kHz) and high voltage (several kV) which causes the formation of a layer whose appearance and structure are very similar to those of p-Si. In this technique the size distribution is very uncertain and difficult to control and the luminescence efficiency is rather poor compared to p-Si.

4.6 Recrystallization of amorphous Si

This technique first start by depositing a layer of amorphous (a-Si) on an SiO_2 substrate by sputtering or PECVD followed by a rapid thermal annealing (RTA) at a temperature between 800 and 900°C for coalescing the nc-Si. [27, 38] Another annealing is necessary in oven with a constant temperature ramp of ~10K/min between 600 and 1050°C to relax the stresses between the two phases nc-Si/SiO_2 and to improve the agglomerated silicon nanocrystals. Just to mention that the amorphous layer recrystallization happens in a typically 60s or lower with the RTA annealing. Furthermore, the thermal recrystallization is controlled by various factors such as the temperatures of annealing by RTA and the temperature ramp speed of the post-annealing. This technique produces size distributions relatively easy to control but is limited on the minimum size of nc-Si (~ 2.5 nm) due to the stress. The obtained luminescence yields from nc-Si obtained by this method are rather low compared to the one obtained from p-Si.

By comparing the different techniques presented in this section, we conclude that the ion implantation and LPCVD show a very clear advantage over other techniques, particularly in terms of degree of control of the size distribution of the nc-Si and the luminescence efficiency obtained on the nanostructures. Moreover these two techniques are particularly compatibility with the technological methods of the current microelectronics.

5 Origin of luminescence of nc-Si

The luminescent properties of nc-Si are the great interest of the scientific community and their origin caused an intense debate among researchers so, many theories and models were proposed to date. In fact, it will be beneficial to expose the origin of luminescence of silicon nanocrystals through the suggested models.

In General, the luminescence in most of nc-Si is characterized by:

- Broad emission spectrum (200-300meV).
- Long time decay for the luminescence (~μs at RT and ~ms a low temperature) with a multi-exponential character.
- Abnormal behavior of PL versus temperature with a maximum around 100K.
- Existence of TO and TA signals in the resonant PL spectrum for silicon nanocrystals passivated with hydrogen.
- Energy shift between absorption and emission (stocks shift) that can reach ~1 eV.
- Loss of energy intensity and position of PL signal in IR and red range for silicon nancrystals annealed under oxygen atmosphere.

Thus, an acceptable model should be able to explain all these features convincingly. Most models made up to date can be classified in 6 major groups [39-41] summarized in the Figure 8. But no studies have clearly demonstrated the dominance of one of these particular processes in observed PL spectra.

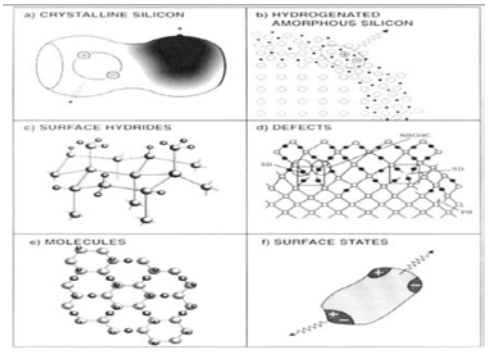

Figure 8: Illustration of the 6 models proposed for the origin of luminescence in nc-Si: a) Quantum Confinement, b) hydrogenated amorphous silicon, c) surface Hydrides d) Defects in SiO2, e) siloxane and f) interface states.

A brief explanation for each model is given in the following sections to highlight its strengths and weaknesses for luminescence in nc-Si.

5.1 Quantum confinement model

This model was proposed first in 1900 by Canham *et al.* [8] to explain the visible photoluminescence of p-Si and in 1997 Estes *et al.* [42] provided the first experimental evidence in its favor. According to this model the reduction in size of the lattice causes a quantum confinement of carriers and this confinement increases the energy gap which can break the rule of selection of the vector of wave k allowing the optical transitions without the intervention of phonons.

For example, the confinement in one dimension (that produces a 2D structure called potential well structure of thickness L) of an exciton produced a band gap ε_g^*:

$$\varepsilon_g^* = E_g + \frac{1}{L^2}\left(\frac{1}{m_e^2} + \frac{1}{m_h^2}\right)\frac{h^2\pi^2}{2} \qquad (4)$$

Where, m_e and m_h are respectively the effective masses of the electron and the hole forming the exciton and E_g is the width of the band gap of the semiconductor. [11] Furthermore, this confinement of charged carriers causes a "relaxation" of the conservation rule of momentum, which requires in particular case of a semiconductor with indirect gap, such as silicon, where a phonon participate in recombination of a electron-hole pair. In fact, the

confinement in the space of the pair of electron-hole emphasizes its spatial location, which, under the principle of uncertainty ($\Delta x \cdot \Delta k \geq 1/2$) results in a broadening of the accessible values of wave number k. Thus, the quantum confinement promotes the excitons recombination within nc-Si relative to the case of crystalline Si.

When a radiative recombination occurs, the energy emitted in the form of a photon E_{ph} is given by:

$$E_{ph} = E_g - E_b + \Delta E \qquad (5)$$

where E_g is the gap energy of the crystalline material, E_b is the binding energy of exciton, et ΔE is the increase in energy of the gap due to the quantum confinement.

According to the simple theory of the effective mass, ΔE is connected to diameter of nc-Si by the equation:

$$\Delta E = \frac{c}{d^2} \qquad (6)$$

where c is an appropriate constant and d is the diameter of the nc-Si. A model describing the spectral emission distribution of a set of nc-Si as function ΔE was developedin 1996 by Chen *et al.* [43]. In this model, we consider the PL emitted by a set of nc-Si with diameters following a Gaussian distribution P(ΔE) with average do and standard deviation σ. then the emission probability as a function of gap increasing P (ΔE) is:

$$P(\Delta E) = \frac{K}{\Delta E^3} exp\left\{-\frac{1}{2}\left(\frac{d_o}{\sigma}\right)^2\left[\left(\frac{\Delta E_o}{\Delta E}\right)^{1/2} - 1\right]^2\right\} \qquad (7)$$

where K is the normalization constant. Thus, using (5) and (7), it becomes possible to predict the PL emission spectrum P(σ) of the Gaussian distribution of nc-Si with a known average diameter do and standard deviation σ. (see figure 9) The typical value of E_b is 0.08 eV, although it was estimated that it depends exponentially on the nc-Si, diameter from 0.05 eV (d = 10 nm) to 0.24 eV (d = 2 nm). [44]

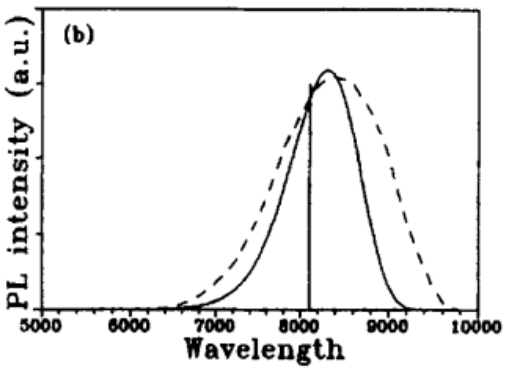

Figure 9: Comparison between the experimental (dashed line) and theoretical (solid line) for PL intensities in arbitrary units as a function of the wavelength. The vertical line shows the position of the theoretical PL peak with σ = 0 A. [43]

To explain the multi-exponential decay time of the photoluminescence, the quantum confinement model postulates that a wide variety of sizes and nanocrystals of different forms (and therefore with different oscillator strengths) emit at considered special energy. Furthermore, from the Figure 10 is considered that the time decline of the luminescence consists in two different lifetimes (singlet and triplet lifetime) according to the states of the excitons. Thus, while on one side the life time of the singlet state (σ_s) is of order of

microseconds which coincides with the theoretical predictions [45] and decreases with the size of the nanocrystals, the lifetime of the triplet state (σ_t) is of the order of ms. In principle it should be infinite but it becomes weak due to the interactions spin-orbit of the electrons that mix a portion of the singlet character of the triplet.

Moreover, to explain the unusual behavior of the photoluminescence as function of temperature, the model assumes that the optical absorption takes place preferentially in the singlet state rather than in the triplet state. Thus, at low temperatures when the thermal energy of carriers is very low compared to the energy of separation of the exciton states, the photogenerated carriers in the singlet state will relax to the triplet state by recombining with a longer life time (~ ms) and therefore a lower photoluminescence intensity.

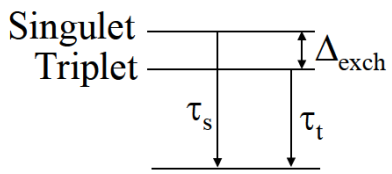

Figure 10: Scheme of separation of the exciton in Singlet and Triplet states.

This model explains adequately the most emission characteristics for nc-Si such the width of the spectrum, the long time of recombination, the behavior of the photoluminescence with temperature as well as the existence of signatures of TO and TA phonons in resonant photoluminescence spectrum. However it cannot explain appropriately the huge Stokes shift and the quasi-independent of energy position to the nanocrystals size for diameters less than 3 nm after annealing in oxygen.

5.2 Hydrogenated amorphous silicon model

This model was proposed by Sebille *et al.* [46] by considering the origin of photoluminescence comes from the hydrogenated and disordered phase created during the fabrication process of nc-Si. In fact, The model explains the luminescence characteristics through extrapolation with those known for the visible band of the hydrogenated amorphous silicon [47], which allows to explain the particular width of the emission spectrum as well as the long recombination time that differs from a typical exponential of disordered systems. [48] This model is no more valid since an annealed sample under oxygen at temperatures 900°C or above does not contain hydrogen and still emit without any shift in the position of the luminescence. In addition, the model is unable to explain the phonons signatures and Stokes shift.

5.3 Model surface hydrides

This model was proposed by Prokes *et al*. [49] and considers that the molecules Si-H_x are the origin of the luminescence. Thus, according to the calculations of the band structure obtained by Prokes using the tight-binding method, the chain of polysilane (Si-H_2)n may give a material with an gap energy E_g greater than that of crystalline Si.

This model succeed to explain the very high loss of luminescence caused by hydrogen desorption on the surface of the p-Si freshly prepared and annealed. But it cannot explain the photoluminescence of nc-Si passivated by elements

other than hydrogen, and in particular those passivated with oxygen.

5.4 Siloxanes Model

This model was proposed by Brandt *et al*. [41] and suggests that only siloxane is responsible for the luminescence of nc-Si. It provides a possible explanation for the very broad luminescence spectrum (~ 300meV) in the visible - near infrared (600nm ~ 800nm), the multi-exponential decay in time for the PL components (order of ms at 300K) and the dependence of the PL intensity with temperature (with a maximum PL intensity located between 50K and 90K). However this model is unable to explain the persistence of the photoluminescence on the nc-Si subjected to annealing at temperatures above the critical temperature for decomposition of siloxanes and other molecules.

5.5 Defects Model in SiO_2

In 1993 Sacilloti *et al*. [50] proposed a mechanism called recombination "type II "to explain the luminescence of nc-Si by proposing that electrons location before and after the radiative recombination is carried out in two different materials, especially Si and SiO_2. Indeed, the gap of the SiO_2 is in the range of 9eV, it can be so reasonable the existence of energy levels within the gap. Thus, while many of these levels will be located near the edge of the conduction band of Si others will locate near the edge of the valence band. So, the excited electrons from the valence band to the conduction band or conversely can thus relax non-radiatively to these sub-levels, and from there they can recombine radiatively.

With this model it is possible to explain the huge Stokes shift for nc-Si with diameter less than 3 nm passivated in oxygen. But it cannot explain the energy blue shift of the luminescence of the p-Si after a simple modification of etching conditions also it cannot explain the phonon signatures observed in the resonant PL characterization of nc-Si passivated with hydrogen and their absence on the nc-Si passivated with oxygen.

5.6 Interface states Model

The model of interface states was proposed by Koch *et al*. [51] and explained the lack of dependence between the size of nc-Si and the PL energy for various groups including the oxidized nc-Si. [52-54] This model uses the quantum confinement model that consider that the absorption takes place in the heart of nanocrystallites and that the luminescent emission occurs through the electronic defects which form states at the interface of nc-Si and the surrounding matrix. The main difference with the defects model in SiO_2 lies in the assumption that the radiative recombinations are performed through the states of defects in nanocrystals and not through defects in the SiO_2 matrix. The model establishes that the atoms at the surface of the silicon nanocrystals arrange themselves according to a local structure which causes variations in the length and the angle of Si-Si. These variations depend on the specificity of the local chemical composition and allow the formation of a series of electronic states in which the

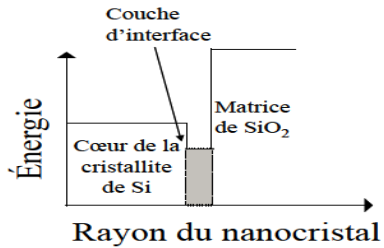

radiative transitions take place. In the same context, Kanemitsu *et al.* [55] proposed a more complete model, called the 3 regions (shown in Figure 11) namely, the silicon nanocrystals, the transition layer at and the surrounding matrix of SiO_2.

Figure 11: Interface states Model scheme showing the three regions.

The optical absorption occurs therefore within the nc-Si and the excitons are formed then migrate to the n-Si interface layer /SiO_2 by a thermal process and are finally in this localized state of the radiative recombination where will take place. Just to mention that if the size of the nanocrystal is above a certain critical radius the excitons will remain in the nanocrystal and the recombination occurs inside. In contrast, if the size of nc-Si decreases beyond a critical radius, the excitons are confined in the interface region and the radiative recombination will take place with a lower energy to the energy gap of the nanocrystal.

Moreover, according to Kanemitsu *et al.* the excitons cannot be located in a defect within the nc-Si because usually these defects act as nonradiative centers

This model explains the most experimental observations of the luminescence of nc-Si such as the Stokes shift and the time decay of the PL energy. But it cannot explain the observation of phonons signatures on p-Si or nc-Si and also unable to explain the very good agreement between the experimental values and theoretical predictions of the PL energy when the nc-Si are passivated with hydrogen.

5.7 Quantum confinement model + interface states

Recently, a new model that reconciles the two Accepted models namely the quantum confinement with that of the interface states. This model was proposed by Wolkin *et al.* [56] in 1999 and considers the role of oxygen in the luminescence of p-Si and highlights the importance of the passivating element of the surface of nc-Si. According to this analysis, if the surface is passivated under hydrogen atmosphere, the radiative recombination will be through the free excitons within nanocrystals and the PL energy will be equal to the excitonic gap. In this case the model of quantum confinement adequately explains the nc-Si luminescence. However, if the passivation is under oxygen atmosphere, the process is complicated since the electron is trapped (within a few picoseconds) in the localized states of the surface (caused by the Si = O) and the radiative recombination will give less PL energy than the excitonic gap. In this case the model of interface states is used to explain the luminescence.

These two mechanisms were illustrated by Kanemitsu [57] in their recent publication in the figure 12.

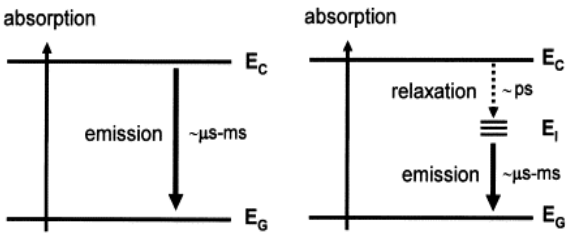

Figure 12: Optical transition for nc-Si passivated a) with Hydrogen b) with Oxygen. [57]

Figure 13 summarizes the results of theoretical calculations of the PL emission energy as a function of particle size for nc-Si. The grey curve corresponds to the first approximation of quantum confinement. [8]

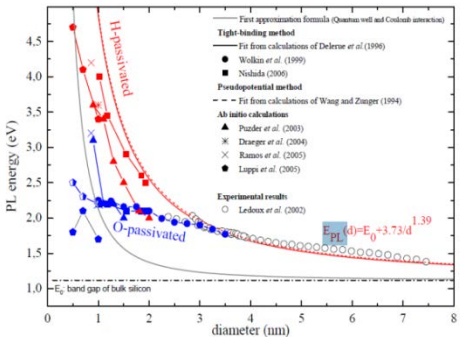

Figure 13: Theoretical and Experimental results of PL emission energy of free nc-Si as a function of the size from Ledoux *et al.* [58]

The red and the blue curves correspond to the theoretical calculation for samples passivated with hydrogen or oxygen respectfully. It is generally admitted that theoretical results of H-passivated nc-Si evaluated by tight binding method, [59-62] which are in a good agreement with those evaluated by the pseudopotential method that are the most accurate. [63] In addition to the theoretical work, Ledoux *et al*. [58] showed that the experimental results (displayed in black open circles) fit well with the theoretical calculation.

6 Techniques for Characterization of Silicon Nanocrystals

The characterization of synthesized silicon nanocrystals is a crucial problem because the analysis techniques with a resolution or sensitivity enough for the characterization of nc-Si are relatively limited. The most techniques used in this research field such as transmission electron microscopy (TEM), X-ray photoelectron spectroscopy (XPS), photoluminescence (PL) spectroscopy Raman spectroscopy, infrared spectroscopy in Fourier transform (FTIR), ellipsometry spectroscopic or the X-ray diffraction (XRD) are universally recognized and used directly or indirectly to understand the various properties of nc-Si.

The purpose of this section is to briefly present the most used techniques to analysis the nc-Si.

6.1 Electron microscopy

For many applications it is essential to obtain a direct image of the synthesized nc-Si. [64] Thus, the scanning electron microscopy (SEM) and transmission (TEM) are used for this purpose and provide information on the morphology, the arrangement and the structure of nc-Si.

6.1.1 Scanning electron microscopy (SEM)

Scanning electron microscopy (SEM) was used to characterize quickly and effectively the LPCVD deposited nc-Si. The deposited nc-Si monolayers are indeed not encapsulated in a matrix but left in the open air. The nc-Si therefore has a relief which allows the characterization in planar view with a reduced time preparation. The figure 14 shows SEM image that was taken by a High-resolution scanning electron microscope (SEM) with field-emission electron source (Carl Zeiss Leo 1530). The SEM has a theoretical resolution of 1nm with an acceleration voltage of 20kV and can perform magnifications up a million times (1000 kX). According to the figure the size of the deposited

nc-Si by a conventional RF-PECVD reactor is very small and have a radius bellow 5 nm. [65]

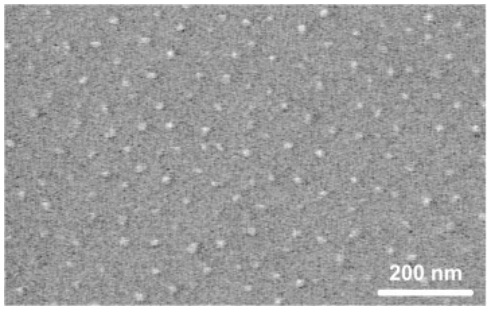

Figure 14: Plane-view SEM image shows that only regions with higher densities of silicon nanocrystals with dimensions of about 3–4 nanometers. [65]

6.1.2 Transmission electron microscopy (TEM)

The transmission electron microscopy (TEM) is a powerful technique for the imaging the silicon nanocrystals. TEM works on the same principle as the optical microscopy with differences in the wavelength of the electron beam compared with the visible light. To allow transmission of electrons through the sample, the latter must first be prepared as a thin plate by a chemical or mechanical etching which makes the TEM a complex and difficult technique to implement. The various techniques of visualization used in this work are:

- The high-resolution TEM (HRTEM). (see figure 15.a) Its resolution is high and allows the visualization of the atomic planes of crystalline materials. It proves effectively the presence of nanocrystalline silicon, but only the nanocrystals oriented in the direction of the electron beam will be visible. This technique cannot measure the density of nc-Si in the matix. [66]

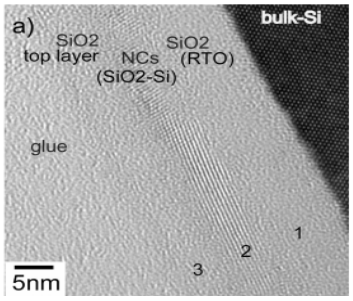

- The energy filtered TEM (EFTEM) (see figure 15.b) allows a chemical analysis of the sample by filtering the incident electron beam so, only electrons with a kinetic energy characteristic of a chemical element are used to form the image. In the case of silicon, the energy of plasmon is around 16.7 eV and is around 21 eV for stoichiometric Si_3N_4 but varies with the alloys composition [66, 67].

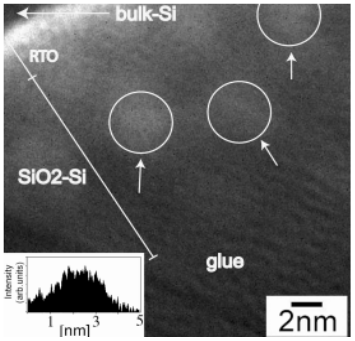

Figure 15: Images of a) HRTEM image, b) EFTEM image, with the plasmon peak of silicon (16.8 eV). [66]

6.2 Infrared absorption spectroscopy (FTIR)

The infrared absorption spectroscopy (Fourier Transformed Infrared Spectroscopy (FTIR)) is a non-destructive technique for determining the nature of bonds present in a material and to quantify them. This technique is based on the interaction between infrared light and vibrational states of matter. When atoms bond to form a molecule, several modes of vibration then become possible. The vibration frequency of these modes tends to occur in the infrared spectra. Thus, each band of the infrared absorption spectrum corresponds to a vibration or rotation that is characteristic of the dipole, making FTIR very sensitive to the chemical composition of the analyzed materials. However, the estimation of the individual atomic species concentration through FTIR is imprecise.

The frequency at which appears a characteristic absorption band of the vibration of a dipole is function of the mass of the atoms involved, but also on the nature of the vibration. Thus, for the same chemical group, modes of vibration appear in of different wavelength. Among the frequently encountered modes, we find the stretching, twisting and swaying modes shown in Figure 16. [68]

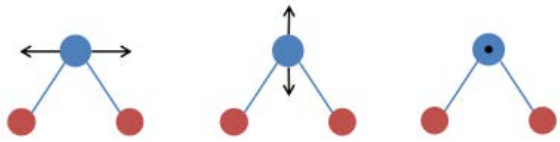

Stretching mode Twisting mode Swaying mode

Figure 16: Principal modes of dipole vibration (SiO2 type). [68]

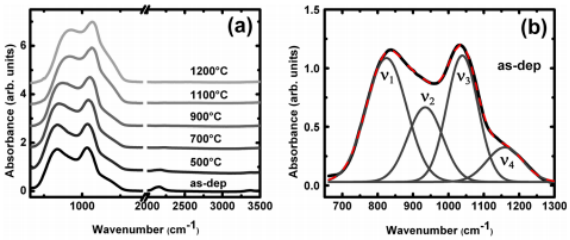

Figure 17 (a) FTIR spectra of the annealed sample at different temperatures; (b) FTIR spectrum of the as deposited sample. [69]

In Figure 17 a) presents the evolution of FTIR spectra of sample at different annealing temperature in which we can clearly see the spectra features around 850, 1050, 2150, and 3350 cm-1. The figure shows also a noticeable decrease with temperature for the intensity of absorption of bands centered at 2150 and 3350 cm_{-1} signature of Si-H and N-H bands respectively [69].

6.3 Raman spectroscopy

Raman spectroscopy is an analytical technique, rapid and non-destructive, it is frequently used to characterize the nc-Si based on the study of the inelastic distribution of light interaction with a material. The Raman effects result from the vibrational transitions due to the interaction between photons coming from a monochromatic source of light and the molecules or atoms of the studied sample. A small amount of these photons (10^{-4}) will be elastically diffused, without energy loss called the Rayleigh scattering and even a smaller amount (10^{-8}) will be inelastically diffused with a slight loss or gain in energy, called Raman scattering respectively Stokes and anti-Stokes.

The Raman spectrum represents the intensity of the scattered light depending on the difference in energy relative to the wavelength of the incident light. The Stokes Raman scattering is always more intense than the scattering spectrum anti-Stokes Raman. This method can be applied to a wide range of materials, gas to solid materials through the liquids. It is more particularly sensitive to Si-Si

bonds and can effectively discriminate silicon crystalline amorphous silicon. However, it does not allow detecting hydrogenated links.

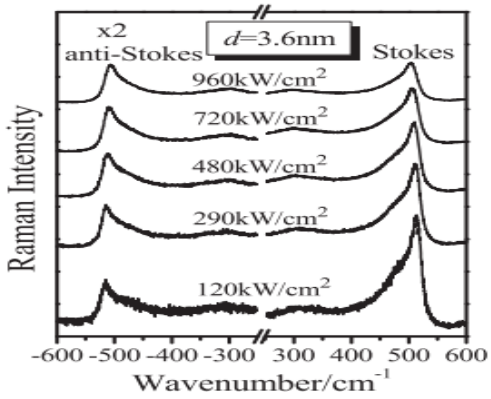

Figure 18: Stokes and anti-Stokes Raman spectra taken from a nc-Si:H with an average Si size of of 3.6 nm under different laser power densities. [70]

The figure 18 shows the typical Stokes and anti-Stokes Raman spectra measured from a nc-Si:H (The average Si nanocrystals size is around of 3.6 nm) for different laser power densities [70]. It can see clearly from the Raman spectra that the broadens of the asymmetrical peaks and the downshifts increase with laser excitation power compared to bulk Si, [71] which means that the Raman spectra of nc-Si:H are sensitive to the laser power density. This can be understood by the poor thermal conductivity of nc-Si:H embedded in an amorphous matrix compared with the bulk Si.

6.4 X-ray diffraction at grazing incidence (XRD)

The *X*-ray diffraction is a non-destructive technique for the characterization structural crystalline materials. Traditionally, this technique is used to Study powders composed of randomly oriented crystals. A beam of X-ray from copper source K_α of a 0.15418 nm wavelength is directed onto the sample with an angle θ and diffracted by the atomic planes of the crystal structure.

The conditions that lead to constructive interference are given by Bragg's law thus requesting the use of the X-ray diffraction at grazing incidence to maximize the path in the layer.

When the samples consist of very small crystals (<100 nm), X-rays are not diffracted at discrete angles and Bragg diffraction peaks are broaden. This enlargement offers an effective method for estimating the size of silicon nanocrystals.

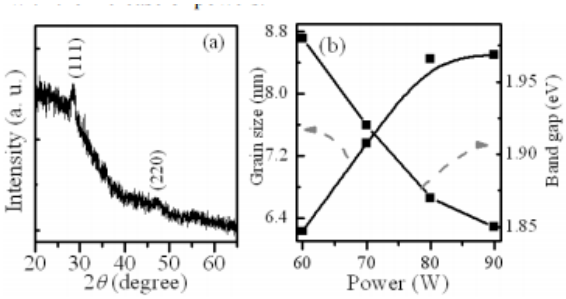

Figure 19: (a) XRD pattern of the nc-Si:H thin films fabricated at 80 W. (b) the power dependent grain size and band gap. [72]

The figure 19 a) shows the XRD measurement pattern of the nc-Si:H thin films fabricated by PECVD at 80 W. Tow peaks are present at $\theta = 14.1^o$ and 23.7^o, that correspond to the orientations of c-Si (111) and (220), respectively. [72] The XRD peak intensity at (111) is very intense which indicates that the nanocrystallites have a preferential grown along the (111) direction. The average size of the silicon nanocrystals is calculated according to the

Debye-Scherrer equation [73] and is shown in the figure 19 b) in which the average size of the silicon nanocrystals increases with the powers and is ranging between 6.0 and 8.4 nm.

6.5 Time-resolved photoluminescence

Photoluminescence spectroscopy (PL) is a widely used technique to study the light emission from nanostructured materials. The PL is based on the excitation of the sample using a monochromatic source that excites electrons from the valence band to the conduction band energy levels. The photo-excited electrons relax to the edges of the conduction band or to the radiative centers before recombining and returning to a lower energy level while emitting a photon. In theory, the photoluminescence can be used to determine the optical gap of a material provided that the excitation energy is large enough to excite an electron from the valence band to the conduction band. However, the observed photoluminescence may also result from defects in the layer whose energy levels are lower than the band edges. The result is then a gap between the emission energy and the energy of absorption threshold called Stokes shift.

Since the discovery in 1990 by Canham of the intense luminescence from the porous silicon subjected to an optical excitement [8] an impressive number of scientific publications have been devoted to the PL of the nc-Si. It is generally found that the PL spectrum of nc-Si is between 600 and 1000 nm (1.24 to 3.11 eV), and it has a substantially a Gaussian shape (slightly unbalanced), with a mid-height width of 200 to 300 meV. A portion of this spectrum is in the visible region, and it is actually possible to see it with naked eye in the best conditions. Also, the energy difference between the excitation beam and the PL emission (called the Stokes shift) can easily reach or exceed 1eV.

It was observed also that the intensity of the PL of nc-Si depend on temperature as shown in the figure 20, the spectra become slightly narrower and shift to the blue. This effect has been reported and explained by the model introduced by Calcott et al. [74] and that the oxidation of nc-Si causes a decrease in intensity and redshift (Low energy) of the PL spectrum. [56]

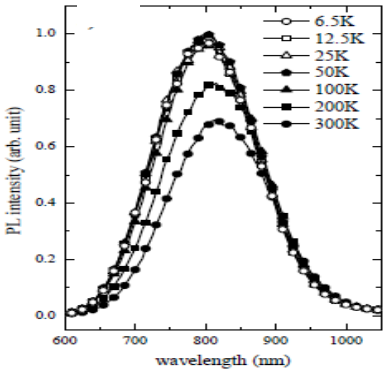

Figure 20: Temperature dependence of the PL spectra of nc-Si embedded in SiO2 [74]

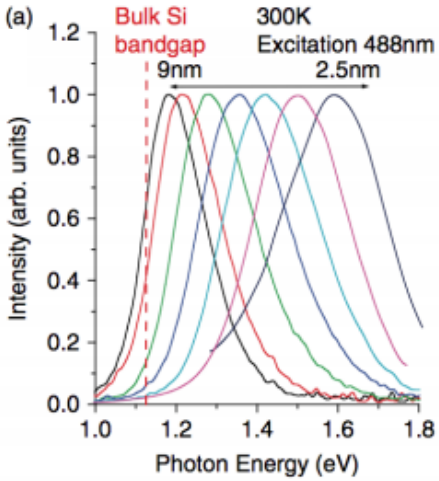

Figure 21: PL spectra at 300K for silicon nanocrystals embedded in SiO2 matrix. [75]

The figure 21 shows different spectra corresponding to different sizes of silicon nanocrystals ranging from 2.5 to 9 nm. [75] The spectra were recorded at room temperature under an excitation at 488 nm. The band gap of the bulk silicon is represented by a line vertical red dotted line. The photoluminescence of silicon nanocrystals is shifted to high energies when the nanocrystals size decreases. This suggests that the size change induces a change in the energy levels of nanocrystals compared to bulk silicon. The full width at half maximum important spectra is mainly attributed to the size distribution of silicon nanocrystals. Sychugov *et al.* [76] were able to measure the photoluminescence of a single nanocrystal and they showed that the width at mid-height of it is very low (about 20 meV at 80 K). In terms of PL life of time is very long and is of order of a few microseconds at room temperature to a few ms at low temperatures (T ~ 2 K). [77, 78]

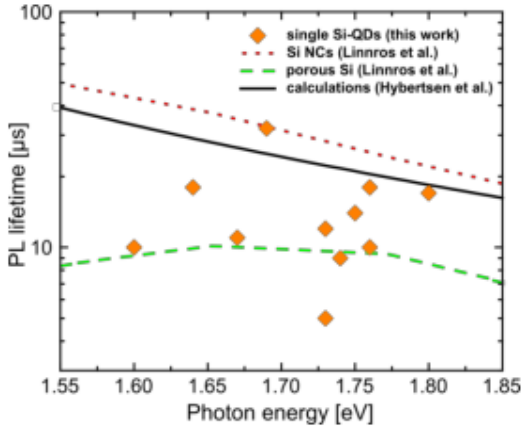

Figure 22: Room temperature PL lifetimes of single silicon nanocrystals versus photon energy at a laser power density of 25 Wcm^{-2} [79] as well as theoretical calculations given by Hybertsen et al. [80] (red and green dashed lines, and black solid line, respectively) are plotted for comparison.

The PL lifetimes of a number of single silicon nanocrystals are shown in the figure 22. The random distribution of PL lifetimes has a relatively broad range versus the emission energies, suggests a strong influence of other parameters than nanocrystal size, passivating molecules, geometrical shape, possible defect sites, and the recombination rate of the PL in silicon nanocrystals. [79]

7 SILICON NANOCRYSTALS APPLICATIONS

7.1 Microelectronic applications

The steady decline in the size of integrated circuits for the past forty year helped to reduce drastically the manufacturing costs and the increase of performance of microelectronic systems. This development is based on the miniaturization of the microelectronic circuits: the MOS transistor. The Number of transistors passed from thousand to several million per chip and has followed the technological advances and Moore's Law [1], which predicts a doubling of the number of transistors in the same surface every 18 months. Thus, a dimension of 10 µm en 1970, for a MOS transistor is decreased to a size smaller than 0.1 µm today. If this evolution continues at the same rate, it will be of the order of ten nanometers in one or two decades. For such small sizes, some fundamental physical limits will be reached and will prevent the operation of the devices such as leakage by tunneling through the gate oxides, and fluctuating of numbers of dopants in the channel

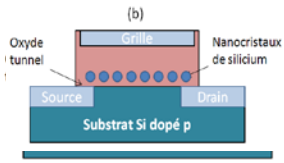

…etc. It is therefore necessary to find new solutions to the high degree of integration in order to improve the existing technologies.

7.1.1 Flash memory in silicon nanocrystals

Flash technology is used as basic cell for MOS transistor having a floating gate buried in the middle of the gate oxide between the channel and the gate (Figure 23 a). A floating gate is a semiconductor layer insulated by a dielectric material. The loading/unloading of the grid is performed by passing electrons through the tunnel oxide tunneling effect (assisted by defects in the insulation). At rest, all the charges present in the floating gate are trapped, thereby to store information. The transistor threshold voltage is then proportional to the number of charges stored in the floating gate: it is the memory effect. To ensure time retention greater than 10 years, the thickness of the tunnel oxide must be greater than 8 nm. So, a greater voltage of 17 V is needed to program the memory and thus the operation is limited to 10^5 cycles due to degradation of the oxide and of the effect of the hot electrons. If the tunnel oxide was less than 2 nm, the programming voltage V is reduced to 4 [81]. This would then reduce the power consumed by the microcontroller as well as the dimension of its components limited by the high voltage currently used. In addition, for a tunnel oxide layer of 2 nm, the passage of carriers is by done by direct tunnel effect rather than the process of conventional Fowler-Nordheim. [82] Therefore it can be expected a faster rate of writing/ reading and longer. So, for these Flash memories the challenge is to reduce the thickness of the tunnel oxide while maintaining a 10-years retention time.

Many electrical studies on silicon nanocrystal memories show promising characteristics as candidates for future deep-submicron non-volatile memories (see figure 23 b). [5, 83-90] Recently, in 2010, the first industrial flash memory based on silicon nanocrystals notably been achieved by ATMEL Corp. [91] This flash memory was obtained by chemical vapor deposition (CVD) and using the technological processes for fine engraving of 90 nm to achieve about 200 nanocrystals by bit. These new memories require less current for programming, and the time for writting is about 100 microseconds, which is ten times faster than the conventional Flash memories.

Figure 23: Schematic structure of (a) a conventional flash memory and (b) a silicon nanocrystal memory.

The silicon nanocrystals memories have discreet storage for which there storage of one or more electrons in each nanocrystal (depending on the size of the latter). The storage is carried out by tunnel transfer charges (Fowler-Nordheim tunneling, or tunnel Direct) between the semiconductor channel and the silicon nanocrystals through a the oxide tunnel as shown in figure 23 b). The Figure 24 shows the three operating modes are represented (writting, reading and erasing) in the case of a nanocrystal with a single charge.

The operation of writing (storing an electron in a nanocrystal) is done by polarizing the control gate with a voltage equal to the threshold voltage: the drain current decreases and the threshold voltage is shifted. For reading is carried out by evaluating the variation of the current between the states

"stored electron " and "non stored electron". Finally for erasing the memory is performed by applying an equal gate voltage but opposite to the threshold voltage. [92]

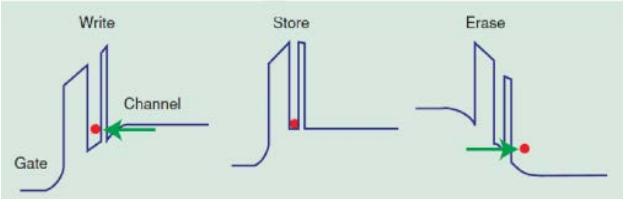

Figure 24: Different states of nanocrystal memory: (a) writing with an electron; (b) storing an electron; (c) deleting an electron (erase). [90]

According to ITRS, 2007 [3], the achievable characteristics of memories based on silicon nanocrystals are:

- Intended optimum dimensions: 18 nm
- Optimal playing time: 2.5 ns
- Time of writing /erasing: 1 s / 10 ms
- Optimal retention time :> 10 years
- Intended writing voltage> 3 V
- Intended reading voltage 0.7 V

Moreover, loading and erasing the memory directly depend on the size nanocrystals and their position relative to the channel. Or the perfect control of both parameters is not feasible experimentally. Therefore, if the inter-nanocrystal distances are low enough a coupling between nanocrystals occurs, which may also influence the memory parameters.

7.2 Optoelectronic Applications

7.2.1 Optical Sources

Silicon is by far the most suitable material for microelectronics. It is indeed an abundant element and has very good electrical, thermal and mechanical properties.

However, it's a poor material for optical applications because of the indirect nature of the electronic gap. Indeed, when a pair electron-hole is created in the bulk silicon, the radiative recombinations producing 1.1 eV photon involves a third particle, the phonon, according to the conservation law of momentum as:

$$h\nu_{photon} = E_g + h\nu_{phonon} \qquad (8)$$

where $h\nu_{photon}$ is the photon energy, E_g the gap g and $h\nu_{phonon}$ is the phonon energy. The emission of a photon from the interaction of three particles (electron-phonon-hole) is less effective as in a direct gap semiconductor that requires only two particles (hole-electron).

The lifetime of radiative transitions that are of the order of 1 ms are too long compared to the lifetime of non-radiative transitions (of the order of microseconds and even of ns), which results in poor optical emission. To overcome this problem, various solutions have been proposed including the silicon nanocrystals that showed a great potential.

In addition to widening the gap, another effect related to quantum confinement in silicon nanocrystals is the increased likelihood of optical transitions as shown in Figure 25.

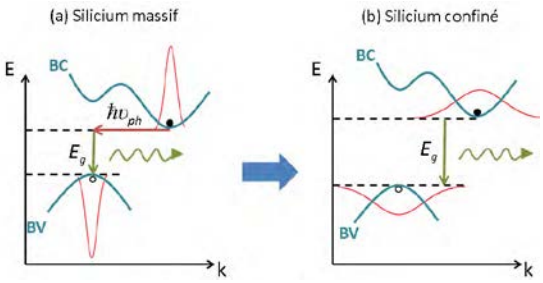

Figure 25: Enlargement of the wave function of the charged carriers confined in the silicon and silicon nanocrystals. [77]

Recent studies shows that silicon nanocrystals are interesting candidates as a light source for silicon based devices. The measurement of the optical gain in the silicon nanocrystals have shown that this could be large enough to allow optical amplification and possibly to obtain a laser effect with silicon nanocrystals. As shown in the figure 26 that presents the first results published in nature journal by Pavesi *et al*. [93] in which net optical gain is seen in both waveguide and transmission configurations and they demonstrated that light amplification is possible using silicon nanocrystals embedded in a silicon dioxide matrix, which open a route to the fabrication of a silicon laser. [93, 94]

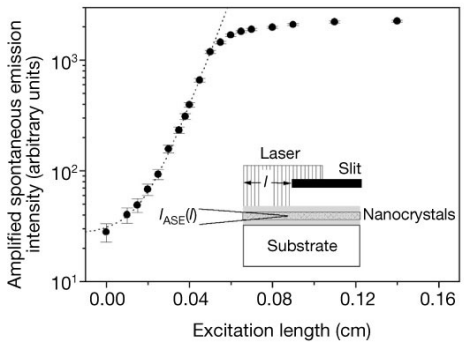

Figure 26: The amplified spontaneous emission with a data fit. The inset shows the VSL experimental method. [93]

7.2.2 Microphotonics silicon

Due to the miniaturization of electronic devices, interconnects within integrated circuits that are currently made from metal lines have certain limitations: signal distortion, power consumption, and signal delay in the lines. It is therefore necessary to develop alternative solutions.

Among the possible solutions, the microphotonics of silicon nanocrystals is a prominent way to solve the problem. This technique consists in transmitting signals in the form of photons in silicon-based micro-wave guides. Photonics makes it possible to create interconnections with considerable bandwidth that is not limited by the resistance, capacitance or stress of the metal lines. [95] In addition to its good optical properties, its low production costs and adaptability to the current microelectronics industry, the advantage of using silicon for photonics is the ability to mix light and electron on the same chip. In particular, nanocomposite layers containing nc-Si offers the opportunity to guide modulate and especially to generate and / or amplify light, which offers prospects encouraging the design of waveguides. [96] In this context, studies have been carried out on silicon nanocrystals waveguides formed of a silicon rich oxide core surrounded by a SiO_2 If envelope. The control and reduction of optical losses in these guides is a necessary condition for the optical gain. Pellegrino et al. reported a Mie scattering (Mie scattering) 2dB.cm^{-1} and direct absorption from 9dB.cm^{-1}. [97]. The same result was reported by the Milgram *et al*. in which they showed that silicon nanocrystals offers a large potential for the integration of optical emission and waveguiding that are compatible for the processing technology.

The figure 27 shows that it's possible from the streak measurement that the couple between the two regions of the chip, and that only ~4dB/cm loss between the two regions for a test device of 100 nm nc-Si layer. A thicker Si-nc film will increase the loss in the emitting region.

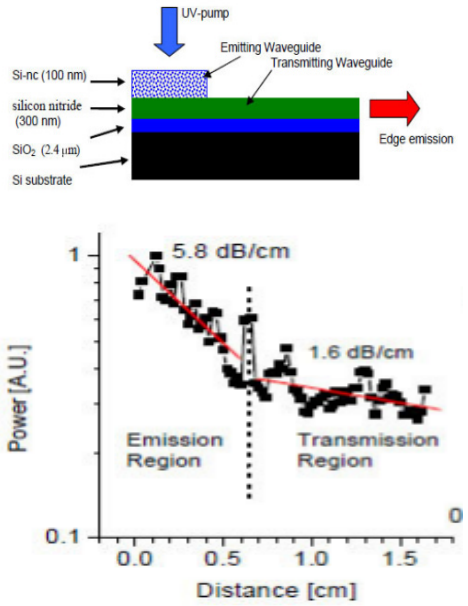

Figure 27: (top) Schematic of a two-sectioned optically pumped Si-nc emitter integrated with a low loss silicon nitride waveguide. (bottom) Streak measurement of a two sectioned chip. Light is prism coupled to the emitting region on the left of the chip and propagates to the right. [97]

7.2.3 Photovoltaic applications

Photovoltaic (PV) cells absorb photons whose energy is greater than the optical gap to create an electron-hole pair. This pair is separated by the electric field created by the p-n junction in the cell and collected by the external electric circuit, thus creating an electric current. Many types of semiconductor materials can be used to fabricate a PV cell. The main feature of these materials is their optical gap that defines the absorbed spectral range. The lower the gap, the higher the number of absorbed photons but the voltage of the external circuit is low. Rather, more the gap is higher the circuit voltage is high but the number of absorbed photons and thus the current generated are low. It is therefore necessary to find a compromise on the value of the gap so that the generated power is the highest possible. For the standard spectrum of the sun, this value is 1.34 eV and the maximum theoretical efficiency of a PV cell ideal for a single energy level is then 33.7%. This is the limit of Shockley-Queisser [98]. However, it is theoretically possible to exceed this limit from two different approaches: the first is to modify the spectrum of the incident light by converting the high or low energy photons into photons of with the most appropriate energy to the cell. The second approach is to introduce a number of energy levels within the PV cell and thus filtering the incident photons. For an infinite number of energy levels, the theoretical limit of efficiency is 68% [99]. In all cases, it is necessary to reduce losses, the maximum efficiency is reached when all the incident photons are absorbed and their energy is fully converted into electricity.

In this context, the concept of third generation PV cell is one of the most innovative approaches. The third generation seeks to exceed the current limits of the first generation cells while keeping the low manufacturing costs of second generation cells based on thin layers, and using non-toxic and abundant materials. Silicon nanocrystals are particularly interesting because of the abundance of silicon and the relatively low cost energy deposition processes of thin layers of Si. Many approaches using silicon nanostructures, such as intermediate cells [100], the multi-carrier generation cells [101] or hot carrier cells [102], cells

based on silicon tandem are the simplest and most promising for future applications. [103]

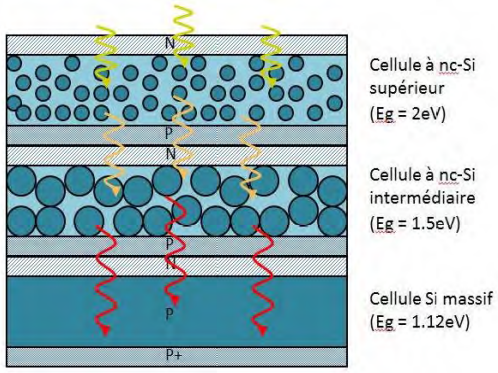

Figure 28: Diagram of a tandem three junctions "all silicon" based on nc-Si as proposed by Green [104].

Conibeer *et al.* [103] has suggested a tandem cell "all silicon" based nc-Si. The cell having three junctions as proposed by Green is shown in Figure 28. Two thin layers of nc-Si are stacked on a conventional Si cell. The actual gap of two higher cells can be adjusted by the size of the nc-Si encapsulated. The theoretical limit of performance for such a cell with three junctions is 47.5%, and the optimal value of the gap is 1.5 eV and 2 eV for the middle and upper cells, respectively [104].

Recently, Dengyuan *et al.* [6] measured the I-V curve of a typical Si-NC:SiC/c-Si solar cell under an illumination level of 100 mW/cm² at 25 °C using the standard AM1.5G spectrum. They found as shown in the figure 29 (top) that the cell has an energy conversion efficiency of 4.66 %. The insert of in the Figure 29 present the I-V curve without the influence of the series resistance which reduce the fill factor from 77 % to 53 %.

In the figure 29 (bottom) shows the EQE and IQE measurements which are high for the blue response than that of a conventional c-Si homojunction solar cell with an IQE is ~ 35 % at 400 nm.

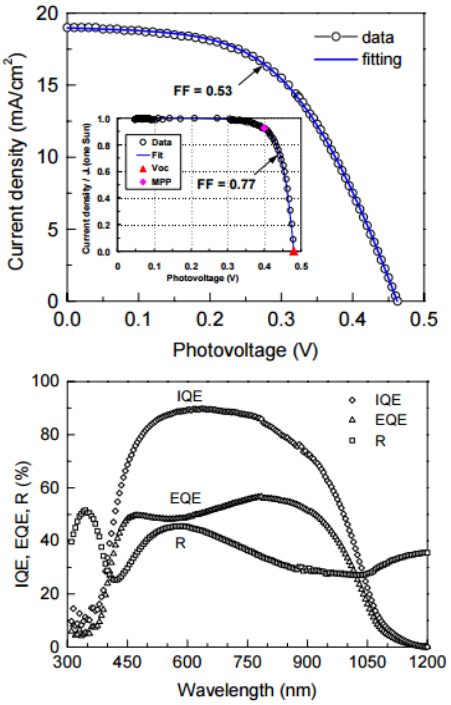

Figure 29: Measured I-V curve (298 K, 100 mW/cm²) (top) and measured reflection (R), external quantum efficiency (EQE) and internal quantum efficiency (IQE) (bottom) for a typical Si-NC:SiC/c-Si solar cell. [6]

7.3 Biophotonic applications

The unique intrinsic optical properties of semiconductor nanocrystals, make them very udeful for photoluminescent probes for biological sensing, imaging and diagnostic applications. [105-108] Silicon nanocrystlas may have advantages in these applications, due to its low cost and low toxicity. However, Si nanocrystals generally have poor colloidal stability in aqueous environments and show unstable photoluminescence.

Recently, Tilley *et al*. have reported the synthesis of water-dispersible silicon nanocrystals with blue luminescence upon anchoring allylamine onto

silicon nanocrystals surfaces [109,110]. Moreover, the group of Erogbogbo *et al* [111] succeeds to obtain water dispersible silicon nanocrystals with blue, green, and yellow photoluminescence by functionalizing them with acrylic acid in the presence of HF. This provides a simple, facile, and straightforward method for the production of colloidally and optically stable water-dispersible Silicon nanocrystals.

The same research group demonstrated the ability of these silicon nanocrystals for imaging of live cancer cells as shown in the figure 30.

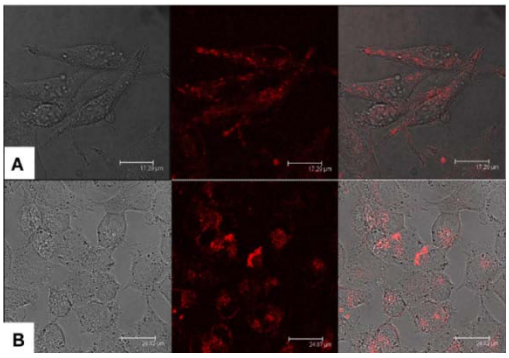

Figure 30: The confocal microscopic visualization of live pancreatic cancer cells treated with a) amine terminated micelle encapsulated nc-Si. b) Tf-Conjugated micelle encapsulated nc-Si. From left to right, the panels show the transmission image, luminescence image, and an overlay of the two. The scale bars are 17.29 μm and 24.87 μm in a) and b) respectively. [111]

Figure 30 a) shows the confocal images of pancreatic cancer cells stained with amine terminated micelle-encapsulated Si nanocrystals and the Figure 30 b) shows the confocal images of pancreatic cancer cells stained with transferrin (Tf)-functionalized micelle-encapsulated Si nanocrystals. Tf was conjugated to carboxyl terminated micelle encapsulated Si nanocrystals, after micelle formation. The micelle encapsulated silicon nanocrystals were found to be strongly taken up by pancreatic cancer cells in vitro, thereby highlighting their potential to be used as a non-toxic optical probe for biomedical diagnostics.

8 Acknowledgments

The authors wish to thank Dr. S. El fitesse for reviewing some parts of the paper.

9 References:

1. [1] G. E. Moore, "Cramming More Components onto Integrated Circuits", Electronics Magazine Vol. 38, No. 8, April 19, 1965.
2. [2] http://www.itrs2.net/
3. [3] ITRS, Interconnect 2007, p. 7, 2007.
4. [4] Dries Van Throuhout, "State of the art in optical interconnect technology", 978-1-4244-5309- IEEE, 2010.
5. [5] Sandip Tiwari, Farhan Rana, Hussein Hanafi, Allan Hartstein, Emmanuel F. Crabbe´, and Kevin Chan, "A silicon nanocrystals based memory", Appl. Phys. Lett. 68 (10), 1996.
6. [6] Dengyuan Song, Eun-Chel Cho, Gavin Conibeer, Yidan Huang, Chris Flynn, and Martin A. Green, "Si Nanocrystals in SiC Matrix for 3rd Generation Photovoltaic Solar Cells", 2007.
7. [7] google scholarship.
8. [8] L.T. Canham, "Silicon quantum wire array fabrication by electrochemical and chemical dissolution of wafers", Appl. Phys. Lett, vol. 57, no 10, p. 1046, 1990.
9. [9] Elinore M. D. de Jong, "Photoluminescence from Silicon Nanocrystals", Master thesis, p 13, July 2012.
10. [10] http://en.wikipedia.org/wiki/Silicium.
11. [11] Ossicini, S., L. Pavesi, and F. Priolo, "Light Emmitting Silicon for Microphotonics", Springer Tracks in Modern Physics, ed. Springer-Verlag. Vol. 194, Berlin, 2003.
12. [12] Jiming Bao, Malek Tabbal, Taegon Kim, Supakit Charnvanichborikarn , James S. Williams , Michael. J. Aziz and Federico Capasso, "Point defect engineered Si sub-bandgap light-emitting diode", Opt. Soc. of Amer, Optics Express 15, 6727-6733, 2007.
13. [13] Canham. L. T, {Silicon quantum wire array fabricaiton by electrochemical dissolution of wafers", Appl. Phys. Lett. 57, 1046-1048, 1990,

14. [14] Shimizu. Iwayama. T, "Visible photoluminescence in Si+implanted silica glass", Journal of Applied Physics, 75(12): p. 7779-7783, 1994.
15. [15] DiMaria.D.J, "Electroluminescence studies in silicon dioxide films containing tiny silicon islands", Journal of Applied Physics, 56(2) p. 401-416, 1984.
16. [16] Richter. A, "Current Induced Light Emission from a Porous Silicon Device", IEEE Electron Device Letters, 12(12): p. 691-692, 1991.
17. [17] Wei-Qi Huang, Shi-Rong Liu, Zhong-Mei Huang, Ti-Ger Dong, Gang Wang, Cao-Jian Qin, "Magic electron affection in preparation process of silicon nanocrystal", Scientific Reports 5, Article number, 9932, 2015.
18. [18] J. B. Xia, "Electronic structures of zero-dimensional quantum wells", Phys. Rev. B, vol. 40, no 12, p. 8500, 1989.
19. [19] A. D. Yoffe, "Semiconductor quantum dots and related systems: electronic, optical, luminescence and related properties of low dimensional systems", Adv. Phys, 50, no1, p. 1, 2001.
20. [20] G. C. John, V.A. Singh, "Porous silicon: theoretical studies", Phys. Rep, vol. 263, no2, p. 93, 1995.
21. [21] C. Bonafos, B. Colombeau, A. Altibelli, "Kinetic study of group IV nanoparticles ion beam synthesized in SiO2", Nucl. Instr. And Meth. B, vol. 178, no 1-4, p. 17, 2001.
22. [22] T. Baron, F. Martin, P. Mur, "Silicon quantum dot nucleation on Si3N4, SiO2 and SiOxNy substrates for nanoelectronic devices", J. of Cryst. Growth, vol. 209, no 4,p. 1004, 2000.
23. [23] H. Seifarth, J. U. Schmidt, R. Grötzschel, "Phenomenological model of reactive r.f.-magnetron sputtering of Si in Ar/O2 atmosphere for the prediction of SiOx thin filmstoichiometry from process parameters", Thin Solid Films, vol. 389, no 1-2, p. 108, 2001.
24. [24] L. Levoska, M. Tyunina, S. Leppävuori, "Laser ablation deposition of silicon nanostructures", Nanostructured Mat, vol. 12, no 1-4, p. 101, 1999.
25. [25] R. E. Hummel, M. H. Ludwig, "Spark-processing - A novel technique to prepare light emitting nanocrystalline silicon", J. of Lum, vol. 68, no 2-4, p. 69, 1996.
26. [26] F. Huisken, B. Kohn, V. Paillard, "Structured films of light-emitting silicon nanoparticles produced by cluster beam deposition", Appl. Phys. Lett, vol. 74, no 25, p. 3776, 1999.
27. [27] L. Tsybeskov, K. D. Hirschman, S. P. Duttagupta, "Fabrication of Nanocrystalline Silicon Superlattices by Controlled Thermal Recrystallization", Phys. Stat. Sol. (a), vol. 165 no 1, p. 69, 1998.
28. [28] B. Garrido, M. Lopez, C. Garcia, "Influence of average size and interface passivation on the spectralemission of Si nanocrystals embedded in SiO2", J. Appl. Phys, vol 91, no 2, p. 798, 2002.
29. [29] M. López, B. Garrido, C. Bonafos, "Phenomenological model of efficient visible emission from Si ion beam synthesised NC in SiO2", E-MRS Spring Meeting, Strasbourg (France), mai 2000.
30. [30] E. Wendler, U. Herrmann, W. Wesch, "Structural changes and Si redistribution in Si+ implanted silica glass", Nucl. Instr. And Meth. B, vol. 116, no 1-4, p. 332, 1996.
31. [31] Ostwald. W, Studien über die Bildung und Umwandlung fester Körper, "Studies on the formation and transformation of solid bodies", Zeitschrift für physikalische Chemie, 22: 289-330, 1897.
32. [32] K. S. Min, K. V. Shcheglov, C. M. Yang, and Harry A. Atwater, "Defect-related versus excitonic visible light emission from ion beam synthesized Si nanocrystals in SiO2", Appl. Phys. Lett. 69 (14), 1996.
33. [33] Timur Nikitin and Leonid Khriachtchev, "Optical and Structural Properties of Si Nanocrystals in SiO2 Films", Nanomaterials, 5, 614-655, 2015.
34. [34] A. Nakajima, Y. Sugita, K. Kawamura, "Si Quantum Dot Formation with Low-Pressure Chemical Vapor Deposition", J. Appl. Phys, vol. 35, no 2B, p. L189, 1996.
35. [35] T. Baron, F. Martin, P. Mur, "Silicon quantum dot nucleation on Si3N4, SiO2 and SiOxNy substrates for nanoelectronic devices", J. of Cryst. Growth, vol. 209, no 4, p. 1004, 2000.
36. [36] M. L. Hitchman, J. Kane, "Semi-insulating polysilicon (SIPOS) deposition in a low pressure CVD reactor", I. Growth kinetics, J. Cryst. Growth, 1981, vol. 55, no 3, p. 485, 1981.
37. [37] X. Y. Chen National, Yongfeng Lu, Y. H. Wu, B. J. Cho, M. H. Liu, "Mechanisms of photoluminescence from silicon nanocrystals formed by pulsed-laser deposition in argon and oxygen ambient", journal of applied physics, volume 93, number 10 , 2003.
38. [38]Zhenyu Wan, Shujuan Huang, Martin A Green, Gavin Conibeer, "Rapid thermal annealing and crystallization mechanisms study of silicon nanocrystal in silicon carbide matrix", Nanoscale Research Letters, 6:129, 2011.
39. [39] R. W. Fathauer,T. George,A. Ksendzov, "Visible luminescence from silicon wafers subjected to stain etches", Appl. Phys. Lett, vol. 60, no 8, p. 995 C. , 1992.
40. [40] Tsai, K. H. Li, J. Sarathy, "Thermal treatment studies of the photoluminescence intensity of porous silicon", Appl. Phys. Lett, vol. 59, no 22, p. 2814, 1991.
41. [41] M. S. Brandt, H. D. Fuchs, M. Stutzmann, "The origin of visible luminescence from porous silicon A new interpretation", Solid State Commun, vol. 81, no 4, p. 307, 1992.
42. [42] M. J. Estes, L. R. Hirsch, S. Wichart, and G. Moddel, "Visible photoluminescence from porous a-Si:H and porous a-Si:C:H thin films", J. Appl. Phys. 82 (4), 1997.
43. [43] Chen. X. S, Zhao. J. J, Wang. G. H, Shen. X. C, "The effect of size distributions of Si nanoclusters on photoluminescence from ensembles of Si nanoclusters", Physics Letters A, 212(5): p. 285-289, 1996,

44. [44] Takagahara. T and K. Takeda, "Theory of the Quantum Confinement Effect on Excitons in Quantum Dots of Indirect Gap Materials", Physical Review B, 46(23): p. 15578-15581, 1992.
45. [45] Haynes, J.R. and W.C. Westphal, "Radiation Resulting from Recombination of Holes and Electrons in Silicon", Physical Review, 101(6): p. 1676, 1956.
46. [46] Martijn van Sebille, Jort Allebrandi, Jim Quik,René, A.C.M.M.vanSwaaij, Frans D. Tichelaar and Miro Zeman, "characterization and density of states determination of silicon nanocrystals embedded in amorphous silicon based matrix", Nanoscale Research Letters, 11:355, 2016.
47. [47] R. P. Vasquez, A. Madhukar, J.A.R. Tanguay, "Spectroscopic "ellipsometry and x-ray photoelectron spectroscopy studies of the annealing behavior of amorphous Si produced by Si ion implantation", J. Appl. Phys, vol. 58, no 6, p. 2337, 1985.
48. [48] K. L. Ngai, K. Murayama, "Luminescence, transient transport and photoconductivity in chalcogenide glasses", Physica B+C, vol. 117-118, no 2, p.118, 1983.
49. [49] S. M. Prokes, O. J. Glembocki, V. M. Bermudez, "SiHx excitation: An alternate mechanism for porous Si photoluminescence", Phys. Rev. B, vol. 45, no 23, p.13788 , 1992.
50. [50] M. Sacilotti, B. Champagnon, P. Abraham, "Properties of type II interfaces in semiconductor heterojunctions, application to porous silicon", J. Lumin, vol. 57, no1-6, p. 33, 1993.
51. [51] Koch. F, V. Petrova. Koch, and T. Muschik, "The luminescence of porous Si: the case for the surface state mechanism", Journal of Luminescence, 57(106): p. 271-281, 1993.
52. [52] S. Veprek, T. Wirschem, M. Rückschlob, "Localization phenomena and photoluminescence in nc-Si and nc-Si/a-SiO2 composites", MRS Symp. Proc. 405-141, Dec. 1995.
53. [53] Y. Kanemitsu, H. Uto, Y. Matsumoto, "Microstructure and optical properties of free-standing porous silicon films: Size dependence of absorption spectra in Si nanometer-sized crystallites", Phys. Rev. B, vol. 48, no 4, p. 2827, 1993.
54. [54] S.M. Prokes, "Light emission in thermally oxidized porous silicon: Evidence for oxiderelated luminescence", Appl. Phys. Lett, vol. 62, no 25, p. 3244, 1993.
55. [55] Kanemitsu. Y, "Light Emission from Porous Silicon and Related Materials", Physics Reports Review Section of Physics Letters, 263(1): p. 1-91, 1995.
56. [56] M.V. Wolkin, J. Jorne, P.M. Fauchet, "Electronic States and Luminescence in Porous Silicon Quantum Dots: The Role of Oxygen", Phys. Rev. Lett, vol. 82, no 1, p. 197, 1999.
57. [57] Y. Kanemitsu, "Efficient light emission from crystalline and amorphous silicon nanostructures", Journal of Luminescence, 100, 209–217, 2002.
58. [58]Ledoux. G, Ehbrecht. M, Guillois. O, Huisken. F, Kohn. B. Laguna. M. A, Nenner. I, Paillard. V, Papoular. R, Porterat. D, Reynaud. C, "Silicon as a candidate carrier for ERE", A&A, Vol. 333, p. 39, 1998.
59. [59] C. Delerue, G. Allan, and M. Lannoo, "Theoretical aspects of the luminescence of porous silicon", Phys. Rev. B Condens. Matter 48(15), 11024–11036, 1993.
60. [60] N. A. Hill and K. B. Whaley, "Size Dependence of Excitons in Silicon Nanocrystals", Phys. Rev. Lett. 75, 1130–1133, 1995.
61. [61] N. A. Hill and K. B. Whaley, "Size Dependence of Excitons in Silicon Nanocrystals - Reply to Comment by Delerue, Lannoo and Allan," Phys. Rev. Lett. 76, 3039, 1996.
62. [62] M. Nishida, "Emission mechanisms of Si nanocrystals and defects in SiO2 materials", Semicond. Sci. Technol., Vol. 21, p. 443-449, 2006.
63. [63] L.W. Wang; A. Zunger, "Electronic structure pseudopotential calculations of large (~1000 atom) Si quantum dots", J. Phys. Chem. 98, 2158, 1994.
64. [64] L. Pavesi, "Silicon Nanocrystals", Wiley-VCH, 2010.
65. [65] F. Karbassian, S. Rajabali, S. Mohajerzadeh, R. Talei, "Room temperature multilayer luminescent silicon nanocrystals", Scientia Iranica, Volume 20, Issue 3, Pages 1063–1066, 2013.
66. [66] Annett Thogersen, Jeyanthinath Mayandi, and Terje G. Finstad, Arne Olsen and Jens Sherman Christensen, Masanori Mitome and Yoshio Bando, "Characterization of amorphous and crystalline silicon nanoclusters in ultra thin silica layers", J. Appl. Phys. 104, 094315, 2008.
67. [67] R. Kärcher, L. Ley, and R. Johnson, "Electronic structure of hydrogenated and unhydrogenated amorphous SiNx ($0 \le x \le 1.6$): A photoemission study", Phys. Rev. B 30, 1896, 1984.
68. [68] W. S. Lau, "Infrared Characterization for Microelectronics", World Scientific Publishing, p81, 1999.
69. [69] A. Zelenina, A. Sarikov, D. M. Zhigunov, C. Weiss, N. Zakharov, P. Werner, L. López-Conesa, S. Estradé, F. Peiró, S. A. Dyakov, and M. Zacharias, "Silicon nanocrystals in SiNx/SiO2 hetero-superlattices: The loss of size control after thermal annealing", Journal of Applied Physics 115, 244304, 2014.
70. [70] Y. Duan, J. F. Kong and W. Z. Shena, "Raman investigation of silicon nanocrystals: quantum confinement and laser-induced thermal effects", J. Raman Spectrosc. DOI 10.1002/jrs.3094, 2011.
71. [71] S. Piscanec, M. Cantoro, A. C. Ferrari, J. A. Zapien, Y. Lifshitz, S. T. Lee, S. Hofmann, J. Robertson, "Raman spectroscopy of silicon nanowires", Phys. Rev. B, 68, 241312, 2003.
72. [72] Donghua Fan and Wenjin Long, "Preparation and multiple exciton generation of hydrogenated nanocrystalline silicon film prepared at different powers", Materials Science and Engineering 87, 012057, 2015.
73. [73] Ahmad Monshi, Mohammad Reza Foroughi, Mohammad Reza Monshi, "Modified Scherrer Equation

to Estimate More Accurately Nano-Crystallite Size Using XRD", World Journal of Nano Science and Engineering, 2, 154-160, 2012.

74. [74] P. D. J. Calcott, K. J. Nash, L. T. Canham, M. J. Kane, and D. Brumhead, "Spectroscopic identification of the luminescence mechanism of highly porous silicon", J. Lumin, Vol. 57, p. 257, 1993.
75. [75] Takeoka. S, Fujii. M, Hayashi. S, "Size-dependent photoluminescence from surface-oxidized Si nanocrystals in a weak confinement regime", Phys. Rev. B62, 16820–16825, 2000.
76. [76] Sychugov. I, Juhasz. R, Valenta. J, Linnros. J, Narrow "Luminescence Line width of a Silicon Quantum Dot", Phys. Rev. Lett 94, 2005.
77. [77] Cullis. A.G, L.T. Canham, and P.D.J. Calcott, "The structural and luminescence properties of porous silicon", Journal of Applied Physics, 82(3): p. 909-965, 1997.
78. [78] Kanemitsu. Y, "Luminescence Properties of Nanometer Sized Si Crystallites Core and Surface States", Physical Review B, 49(23): p. 16845-16848, 1994.
79. [79] Linnros. J, Lalic. N, Galeckas. A, Grivickas. V, "Analysis of the Stretched Exponential Photoluminescence Decay from Nanometer-Sized Silicon Crystals in SiO2", J. Appl. Phys, 86, 6128, 1999.
80. [80] Hybertsen. M. S, "Absorption and Emission of Light in Nanoscale Silicon Structures", Phys. Rev. Lett, 72, 1514–1517, 1994.
81. [81] J. Barbé, L. Xie, K. Leifer, P. Faucherand, C. Morin, D. Rapisarda, E. De Vito, K. Makasheva, B. Despax, S. Perraud, "Silicon nanocrystals grown on amorphous silicon carbide alloy thin films for third generation photovoltaics", PTVC 2012 – Photovoltaic Technical Conference 2012.
82. [82] Fowler. R. H, L. Nordheim, "Electron Emission in Intense Electric Fields", (PDF). Proceedings of the Royal Society A. 119 (781): 173–181, 1928.
83. [83] M. Shalchian, J. Grisolia, G. Ben Assayag, "Room-temperature quantum effect in silicon nanoparticles obtained by low-energy ion implantation and embedded in a nanometer scale capacitor", Appl. Phys. Lett. 86, 163111, 2005.
84. [84] S. Jacob, B. De Salvo, L. Perniola et al, Integration of CVD silicon nanocrystals in a 32 Mb NOR flash memory", Solid-State Electronics 52, 1452–1459, 2008.
85. [85] Wen-Chin Lee, Ya-Chin King, Tsu-Jae King, Chenming Hu, "Investigation of Poly-Si1-xGex for Dual-Gate CMOS Technology", IEEE Electron Device Letters, vol.19, (no. 7): 247, 1998.
86. [86] Z. Liu, C. Lee, V. Narayanan, G. Pei, and E. C. Kan, "Metal nanocrystal memories—Part I: Device design and fabrication", IEEE Trans. Electron Devices, vol. 49, no. 9, pp. 1606–1613, 2002.
87. [87] Z. Liu, C. Lee, V. Narayanan, G. Pei, and E. C. Kan, "Metal nanocrystal memories—Part II: Electrical characteristic, IEEE Trans. Electron Devices", vol. 49, no. 9, pp. 1614–1622, 2002.
88. [88] K. Yano, T. Ishii, T. Hashimoto, T. Kobayashi, F. Murai, K. Seki, "Room-temperature single-electron memory", IEEE Transactions on Electron Devices 41 (9), 1628-1638, 1994.
89. [89] URL http://www.atmel.com.
90. [90] L. Guo, E. Leobandung, S. Y. Chou, "A silicon single-electron transistor memory operating at room temperature", Science 275 (5300), 649-651, 1997.
91. [91] A. Nakajima, T. Futatsugi, K. Kosemura, "Room temperature operation of Si single-electron memory with self-aligned floating dot gate", Appl. Phys. Lett. 70, 1742, 1997.
92. [92] A. Thean and J.-P. Leburton, "Flash memory: towards single-electronics", IEEE Pot., Oct/Nov, pp 35–41, 2002.
93. [93] Pavesi. L, Dal Negro. L, Mazzoleni. C, Franzó. G, and Priolo. F, "Optical gain in silicon nanocrystals, Nature", Vol. 408, p.440, 2000.
94. [94] Fauchet. P.M, Ruan. J, Chen. H, Pavesi. L, Dal Negro. L, Cazzanelli. M, Elliman. R.G, Smith. N, Samoc. M. and Luther-Davies. B, "Optical gain in different silicon nanocrystal systems", Opt. Mater., Vol. 27, p.745, 2005.
95. [95] L. C. Kimerling, "Silicon microphotonics", Appl. Surf. Sci. 159, 8–13, 2000.
96. [96] P. Bettotti, M. Cazzanelli, L. Dal Negro, B. Danese, Z. Gaburro, C. J. Oton, "Silicon nanostructures for photonics", Journal of Physics: Condensed Matter 14 (35), 8253, 2002.
97. [97] P. Pellegrino, B. Garrido, C. Garcia, J. Arbiol, J. R. Morante, M. Melchiorri, N. Daldosso, L. Pavesi, E. Scheid, and G. Sarrabayrouse, "Low-loss rib waveguides containing Si nanocrystals embedded in SiO2", J. Appl. Phys. 97, 074312, 2005.
98. [98] W. Shockley and H. J. Queisser, "Detailed Balance Limit of Efficiency of p-n Junction Solar Cells", J. Appl. Phys. 32, 510, 1961.
99. [99] M. A. Green, "Third Generation Photovoltaics: Advanced Solar Energy Conversion", Springer, 2003.
100. [100] A. Martí, N. López, E. Antolin, E. Cánovas, C. Stanley, C. Farmer, L. Cuadra, "Novel semiconductor solar cell structures: The quantum dot intermediate band solar cell", Thin Solid Films 511, 638-644, 2006.
101. [101] M. C. Beard, K. P. Knutsen, P. Yu, J. M. Luther, Q. Song, W. K. Metzger, "Multiple exciton generation in colloidal silicon nanocrystals", Nano letters 7 (8), 2506-2512, 2007.
102. [102] G. Conibeer, "Third-generation photovoltaics", Materials Today, vol. 10, no. 11, pp. 42–50, 2007.
103. [103] G. J. Conibeer, C.-W. Jiang, D. König, S. Shrestha, T. Walsh, and M. A. Green, "Selective energy contacts for hot carrier solar cells", Thin Solid Films, vol. 516, no. 20, pp. 6968–6973, 2008.
104. [104] Green, M. A., G. Conibeer, I. Perez-Wurfl, S. J. Huang, D. Konig, D. Song, A. Gentle, X. J. Hao, S. W.

Park, F. Gao, Y. H. So, and Y. Huang, "Progress with Silicon-based Tandem Cells Using Group IV Quantum Dots in a Dielectric Matrix", Proceedings of 23rd European Photovoltaic Solar Energy Conference, Spain, 2008.

105. [105] Prasad. P. N, "Introduction to Biophotonics", Wiley-Interscience: Hoboken, NJ, p 616. 4, 2003.
106. [106] Gao. X, Yang. L, Petros. J. A, Marshall. F. F, Simons. J. W, Nie. S, "In vivo molecular and cellular imaging with quantum dots", Current Opinion in Biotechnology, 16, (1), 63-72. 5, 2005.
107. [107]Medintz. I. L, Uyeda. H. T, Goldman. E. R, Mattoussi. H, "Quantum dot bioconjugates for imaging, labelling and sensing", Nat Mater, 4, (6), 435-446. 6, 2005.
108. [108] Wolfgang. J. P, Teresa. P, Christian. P, "Labelling of cells with quantum dots" Nanotechnology, 16, R9-R25, 2005.
109. [109] Tilley. R. D, Yamamoto. K, "The microemulsion synthesis of hydrophobic and hydrophilic silicon nanocrystals", Advanced Materials, 18, (15), 2053-2056, 2006.
110. [110] Warner. J. H, Hoshino. A, Yamamoto. K, Tilley. R. D, "Water-soluble photoluminescent silicon quantum dots", Angewandte Chemie-International Edition, 44, (29), 4550-4554, 2005.
111. [111] Sato. S, Swihart. M. T, "Acid-Terminated Silicon Nanoparticles: Synthesis and Optical Characterization", Chem. Mater, 18, (17), 4083-4088, 2006.

10 CONCLUSION

To continue the historical trend of lowering the manufacturing cost and higher integration density of circuits, it became necessary to resort to new approaches based on silicon nanocrystals to meet the needs of miniaturization are increasingly demanding. Therefore these nanocrystals with a homogeneous and well-controlled size that can be used for the production of devices optoelectronics. In this context, we presented this review paper on the nc-Si aimed to contribute to a better understanding of the optoelectronic properties of this material for its application to electroluminescent devices and the best methods used to fabricate them.

For the fabrication methods for silicon nanocrystals it depends on the objective behind it and the existent facilities in the laboratory. But among all these methods, the ion implantation and LPCVD seem to be the best techniques that allow a better control of the size distribution of the silicon nanocrystals and comparable luminescence yields to those obtained on p-Si. Moreover these two techniques are particularly compatibility with the technological methods of the current microelectronics.

Concerning the subject of the origin of the luminescent in silicon nanocrystals it caused an intense debate and many theories and models proposed to date. But the new model that combines the quantum confinement and the interface states give an adequate explanation of nc-Si luminescence. Still more theoretical works is needed in this area.

Besides the fabrication methods we reviewed the most used technique for silicon nanocrystals characterization. Here again the used techniques depends on the users objectives but the easiest way to characterize the nc-Si is the Photolumenescence since it gives a rapid and reliable results about the emitted light wavelength.

As mentioned in the main text the silicon nanocrystals could be used various applications including flash memory, guiding, modulating and generating, and/or amplifying light and it has a promising feature in the new generation of solar cell devices toward record high converging efficiencies and we are expected to utilize nanostructured materials in biomedical applications since silicon is inert, nontoxic, abundant, and economical.